Simultaneous enhancement of anisotropy and grain isolation in CoPtCr-SiO_2 perpendicular recording media by a MnRu intermediate layer

Jung-Wei Liao,[1] Randy K. Dumas,[2] Hao-Cheng Hou,[1] Yen-Chun Huang,[1] Wu-Chang Tsai,[1] Liang-Wei Wang,[1] Ding-Shuo Wang,[1] Meng-Shian Lin,[1] Yun-Chung Wu,[1] Rong-Zhi Chen,[3] Chun-Hao Chiu,[3] June W. Lau,[4] Kai Liu,[2] and Chih-Huang Lai[1,*]

[1]*Department of Materials Science and Engineering, National Tsing Hua University, Hsinchu 30013, Taiwan*

[2]*Department of Physics, University of California, Davis, California 95616, USA*

[3]*China Steel Corporation, Kaohsiung 81233, Taiwan*

[4]*Materials Science and Engineering Laboratory, National Institute of Standards and Technology, Gaithersburg, Maryland 20899, USA*

(Received 9 January 2010; revised manuscript received 17 April 2010; published 21 July 2010)

We demonstrate using both structural and magnetic analyses that an antiferromagnetic MnRu intermediate layer can simultaneously increase the anisotropy constant and reduce the intergranular exchange coupling of a CoPtCr-SiO_2 recording layer. The anisotropy constant of CoPtCr-SiO_2 is increased by an exchange coupling with the adjacent antiferromagnetic MnRu intermediate layer. Additionally, the MnRu layer leads to better SiO_2 segregation within the recording layer which then weakens intergrain exchange coupling. While the enhanced grain isolation leads to a reduction in the activation volume, a potential loss in thermal stability is avoided due to the enhanced anisotropy.

DOI: 10.1103/PhysRevB.82.014423 PACS number(s): 75.50.Ss, 75.70.Ak, 75.50.Cc, 75.50.Ee

I. INTRODUCTION

Advances in nanomagnetism have profoundly changed information technology, exemplified by the 1000-fold increase in magnetic recording areal density over the past decade.[1] As each bit of information is recorded over an ever shrinking area, thermal stability becomes a critical issue.[2,3] The magnetic anisotropy energy K_uV that stabilizes the magnetization of a magnetic recording bit scales with its volume V, where K_u is the anisotropy constant. At very small bit sizes, the anisotropy will be dominated by the adverse effects of thermal fluctuations. Achieving an *enhanced* K_u in the recording media can compensate for the smaller V in order to maintain thermal stability.[4] On the other hand, when a particular grain switches its magnetization, it affects the neighbors through the intergranular exchange coupling, leading to noises and also masking the intrinsic switching field distribution.[5] A certain number of grains per bit is required to realize a reasonable signal-to-noise ratio. Media with *better isolated grains* are thus highly desirable as they allow each bit to be written over fewer grains, leading to a higher storage density.[6]

In practice, however, it has been difficult to simultaneously accomplish both goals, as a weaker intergranular exchange coupling naturally reduces the thermal stability as well. Currently dual-Ru layers are widely used to promote (0002) texture and achieve well-isolated grains of the recording layer (RL) in CoPtCr-SiO_2 perpendicular recording media.[7] Sputtering of the second Ru intermediate layer (IL) at a high working pressure has been suggested to obtain better grain isolation in the RL. However, poor grain isolation at the interfacial region of the RL near the Ru IL was observed.[8] Doping oxides into the Ru IL to promote the grain isolation in the RL is an alternative method.[9,10] Yet the improvement of the grain isolation during the initial growth of RL has not been clearly demonstrated. Antiferromagnetic (AFM) IrMn has been proposed to keep similar grain size in the RL while enhancing the thermal stability.[11] However, the measured K_u of the RL is not appreciably increased and the enhancement to the RL thermal stability is unclear.[11] In this work, we report an AFM MnRu IL that can simultaneously enhance the K_u of the RL and promote the SiO_2 segregation at grain boundaries during the initial growth of the RL. The reduction in intergranular exchange coupling is balanced by the interlayer exchange bias so that the thermal stability is not compromised.

II. EXPERIMENT

All samples were deposited by using dc magnetron sputtering. The layer structure of the first set of the samples is as follows: Ta (3 nm)/Pt (7 nm)/Ru (10 nm)/Mn_xRu_{1-x} (7 nm)/CoPtCr-SiO_2 (0, 4 or 15 nm)/Ta cap (3 nm). The first IL is a 10 nm Ru layer deposited at 3 mTorr of Ar. The second IL is a Mn_xRu_{1-x} layer, cosputtered from pure Mn and Ru targets at 30 mTorr. Inductively coupled plasma mass spectrometry was used to confirm the composition. The RL was sputtered from a composite CoPtCr-SiO_2 target with 10 mol % of SiO_2. Structural and chemical analyses were performed by x-ray diffraction (XRD), transmission electron microscopy (TEM), and electron-energy-loss spectroscopy (EELS).

Magnetic properties were measured by using a polar magneto-optical Kerr effect magnetometer and a vibrating sample magnetometer. In addition to standard major hysteresis loops, first-order reversal curves (FORCs) are studied, following prior procedures.[12,13] Samples were brought from positive saturation to a particular reversal field H_R, and then the magnetization was measured under increasing applied field H back to saturation, thereby tracing out a single FORC. This process was repeated for successively smaller values of H_R creating a family of FORCs. A FORC distribution was extracted as $\rho \equiv -\partial^2 M(H,H_R)/2\partial H \partial H_R$. By a simple coordinate transformation, ρ was plotted in coordinates of (H_C,H_B), where H_C is the local coercive field and

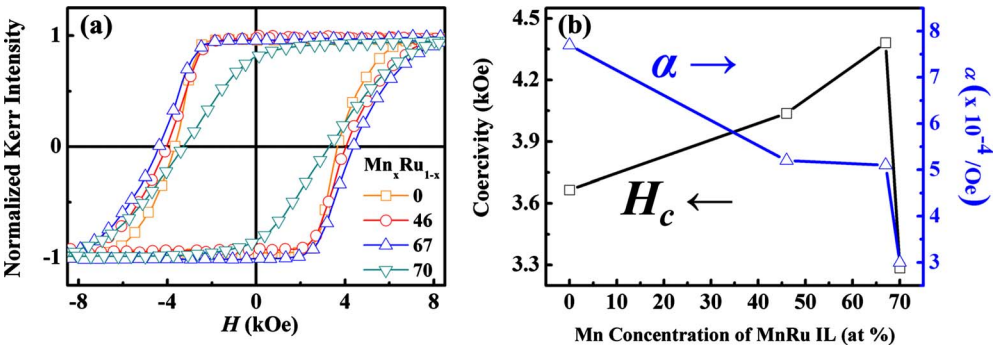

FIG. 1. (Color online) (a) Hysteresis loops of samples with a 15 nm RL grown on different MnRu ILs. The compositional dependence of H_c and α is shown in (b).

H_B is the local interaction or bias field.[12] The K_u and activation volume V_{act} of the RL were investigated by measuring the time-dependent remanent coercivity as follows.[14] After positive saturation the applied field was reduced to a constant and negative value. The time t for the magnetization to decay to zero was recorded and the constant applied field was noted as the corresponding remanent coercivity H_{cr}. The set of data with different reversing fields was fitted with Sharrock's equation: $H_{cr}=H_o(1-\{(k_BT/K_uV_{act})\ln[f_ot/\ln(2)]\}^n)$,[15,16] where H_o is the time-independent intrinsic coercivity, K_uV_{act}/k_BT is the thermal stability factor, f_o is the flip frequency, and n is the response exponent. We chose n and f_o equal to 0.7 and 2×10^{11} Hz, respectively, as previously reported for perpendicular recording media.[17] The K_u and V_{act} of RL are determined from the fitting results. To expose the fundamental interactions present, the ΔM method[13,18] was utilized to obtain $\Delta M(H)=M_{DCD}(H)/M_R+2M_{IRM}(H)/M_R-1$, where $M_{DCD}(H)$, $M_{IRM}(H)$, and M_R are the dc demagnetization, isothermal, and saturation remanence, respectively. $\Delta M(H)$ is expected to be positive for interactions dominated by exchange and negative for those with dipolar origins.

III. RESULTS

The first set of the samples all have the same first Ru (10 nm) IL but different second Mn_xRu_{1-x} (7 nm) ILs. From now on, the comparisons for the RL grown on different ILs are made specifically for the second IL. The θ-2θ XRD scans of the samples with the Mn_xRu_{1-x} ILs of different Mn concentrations all reveal strong Co (0002) texture in the RL. The rocking curves of the Co (0004) peak show that the full width at half maximum for samples on both Ru ($x=0$) and MnRu ILs is nearly the same (3.4°), indicating that the addition of Mn into second IL does not affect the crystalline texture of the RL. In addition, the TEM plan-view images reveal that the grain diameters (without including the grain boundary) of 15-nm-thick RL grown on $Mn_{67}Ru_{33}$ and Ru IL are nearly the same (6.5 ± 1.0 nm).

Hysteresis loops of samples with a 15 nm RL on different Mn_xRu_{1-x} ILs are shown in Fig. 1(a) and the compositional dependence of coercivity H_c and the slope at H_c, $\alpha=\partial M/\partial H|_{H_c}$ are shown in Fig. 1(b). As the Mn concentration x increases from 0 to 67 at. %, H_c increases from 3.67 to 4.38 kOe while the loop squareness remains unchanged. However, further increasing x to 70 at. % results in a decrease in both H_c and loop squareness. Additionally, α decreases with increasing x, indicating reduced intergranular exchange coupling in the RL.[19] Since all the crystalline textures of the RLs on different Mn_xRu_{1-x} ILs are the same, the reduced H_c, loop squareness, and α of the sample with the $Mn_{70}Ru_{30}$ IL might suggest well-isolated grains with reduced grain sizes in the RL.[20]

To investigate the origin of the enhanced H_c and reduced α, the K_u and V_{act} of RLs on $Mn_{67}Ru_{33}$ IL (which has the largest H_c) and pure Ru IL are extracted from fits to the remanent H_{cr}. The K_u of RL on $Mn_{67}Ru_{33}$ IL is $(3.3\pm0.1)\times10^6$ erg/cm^3, which is 27% larger than that on Ru IL, $(2.4\pm0.1)\times10^6$ erg/cm^3. The likely sources for the K_u enhancement are either the exchange coupling between the AFM MnRu IL and the RL or differential segregation of the RL grown on different ILs at the grain boundaries. Furthermore, the activation volume V_{act} of the RL on the $Mn_{67}Ru_{33}$ IL $[(1.3\pm0.1)\times10^{-18}$ cm$^3]$ is reduced by 35% comparing with that on the Ru IL $[(2.0\pm0.1)\times10^{-18}$ cm$^3]$, which indicates better grain isolation in the former sample. The decreased V_{act} is also consistent with the reduced α shown in Fig. 1(b).

To clarify the AFM characteristic of $Mn_{67}Ru_{33}$, we deposited a 10 nm FeCo layer on $Mn_{67}Ru_{33}$. After deposition, the sample was cooled in an in-plane 1.5 kOe magnetic field from 250 °C to room temperature. A clear loop shift is observed with an exchange field of 86 Oe. This unambiguous unidirectional anisotropy is the hallmark of the exchange bias between the FeCo and AFM $Mn_{67}Ru_{33}$.[21] To further investigate the role of the AFM $Mn_{67}Ru_{33}$ and separate the effects of interfacial exchange bias from the differential segregation at grain boundaries of RL, a second set of samples were prepared with the following structure: Ta (3 nm)/Pt (7 nm)/Ru (10 nm)/Ru (7 nm)/CoPtCr-SiO_2 (4 nm)/Ru

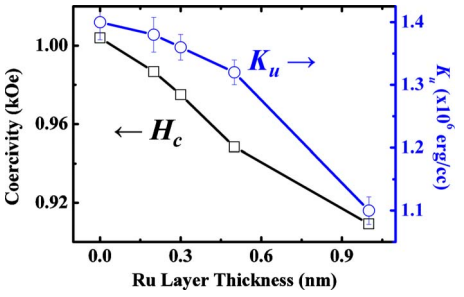

FIG. 2. (Color online) The Ru-layer-thickness dependence of H_c and K_u of the samples with the structure Ta (3 nm)/Pt (7 nm)/Ru (10 nm)/Ru (7 nm)/CoPtCr-SiO_2 (4 nm)/Ru (t_{Ru})/$Mn_{67}Ru_{33}$ (7 nm).

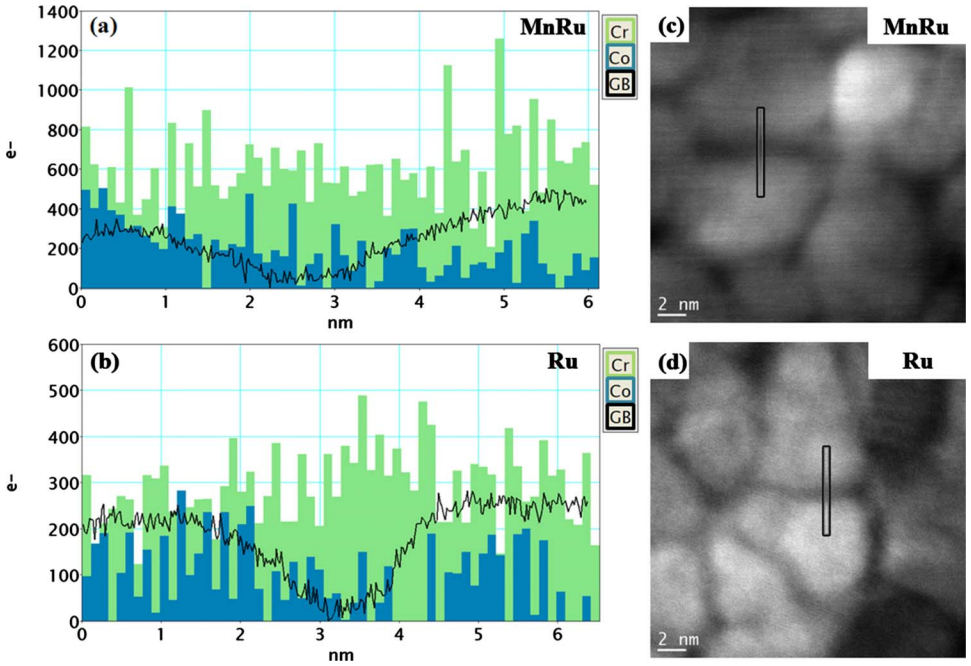

FIG. 3. (Color online) Representative EELS line scans for a 15 nm CoPtCr-SiO_2 grown on 7 nm (a) $Mn_{67}Ru_{33}$ IL and (b) Ru IL, respectively. The corresponding STEM images of the samples are shown in (c) and (d), respectively. The positions of the line scans are shown by the bars in (c) and (d).

(t_{Ru})/$Mn_{67}Ru_{33}$ (7 nm). All the RLs in the second set of samples were grown on the same dual-Ru ILs to ensure the same microstructures in the RLs. A nonmagnetic Ru layer of variable thickness t_{Ru} (from 0 to 1 nm) was purposely inserted between the FM RL and AFM $Mn_{67}Ru_{33}$ IL to probe the interfacial exchange coupling between the two layers.[22] The H_c and K_u decay with increasing t_{Ru}, as shown in Fig. 2, which clearly indicates the enhancement of H_c and K_u by the exchange bias between the FM CoPtCr-SiO_2 layer and the AFM $Mn_{67}Ru_{33}$ IL. Since we deposited $Mn_{67}Ru_{33}$ on CoPtCr-SiO_2 without field annealing, the exchange coupling only contributed to the enhancement of H_c (and effective K_u) instead of the loop shift.[23]

Another potential source of K_u enhancement is the film microstructure. In CoCrPt-SiO_2 type of media, the presence of Cr suppresses K_u; when Cr preferentially segregates at grain boundaries, leading to a low Cr concentration in the middle of the grains, K_u can be enhanced.[6] If this were the origin of the K_u enhancement in the RL grown on MnRu, we should observe a relatively higher Cr concentration (1) at grain boundaries vs inside the grains; (2) in the sample grown on MnRu vs that grown on Ru. To clarify this issue, we have performed EELS analysis using scanning-TEM (STEM) on the first set of samples with a 15 nm RL on top of both $Mn_{67}Ru_{33}$ and Ru ILs. The representative EELS line scans, along with the corresponding STEM images and positions of the line scans for the samples with $Mn_{67}Ru_{33}$ and Ru ILs are shown in Figs. 3(a), 3(c), 3(b), and 3(d), respectively. Through numerous scans we find that while the Co concentration does decrease at grain boundaries, the Cr concentration (~6 at. % in the samples) is essentially uniform across the grains, as well as at grain boundaries. In particular, the relative Cr concentration at grain boundaries in the MnRu sample [Fig. 3(a)] is no higher than that in the Ru sample [Fig. 3(c)]. These results argue against the possibility that the enhanced K_u is purely microstructural in origin. Although subtle microstructural differences may still contribute to the K_u enhancement, this effect is clearly secondary to the exchange bias contribution.

To investigate the origin of the V_{act} reduction, we have analyzed the microstructure of the IL without a RL. Figures 4(a) and 4(c) show the TEM plan-view images of $Mn_{67}Ru_{33}$ and Ru ILs, respectively. The average grain sizes of the $Mn_{67}Ru_{33}$ and Ru are about the same (5.6 nm) but relatively thick grain boundaries are clearly observed in the $Mn_{67}Ru_{33}$ IL. The thick grain boundaries of the $Mn_{67}Ru_{33}$ IL should promote the formation of an isolated domelike structure, and the subsequent SiO_2 segregation at the grain boundaries of RL.[9] To test this idea, we have deposited a thin 4 nm RL on 7-nm-thick $Mn_{67}Ru_{33}$ and Ru ILs. Plan-view TEM images

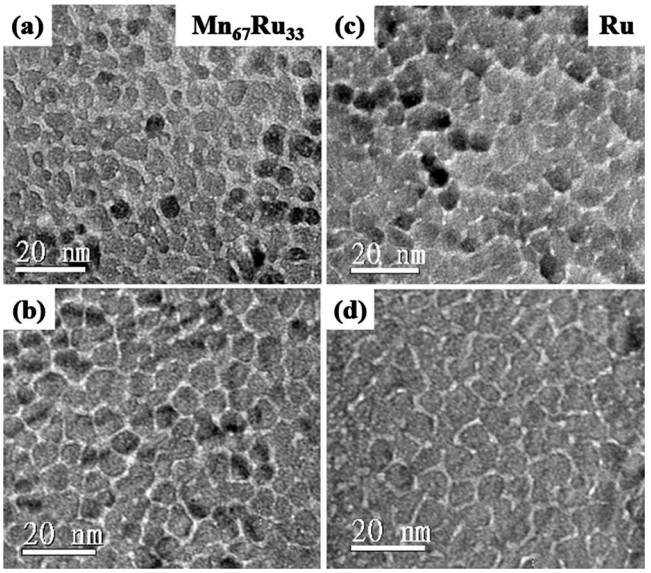

FIG. 4. TEM plan-view images of $Mn_{67}Ru_{33}$ and Ru ILs are shown in (a) and (c), respectively. Similar images of samples with 4 nm of RL grown on $Mn_{67}Ru_{33}$ and Ru IL are shown in (b) and (d), respectively.

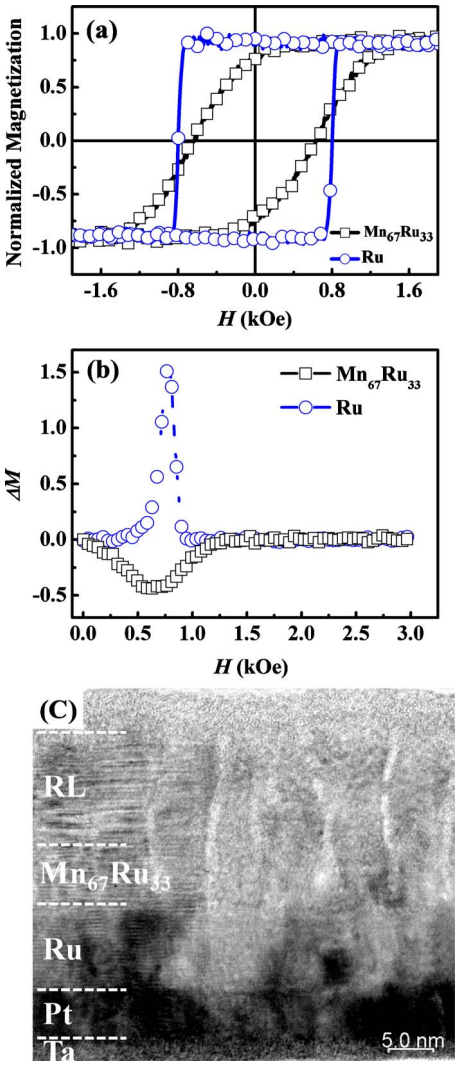

FIG. 5. (Color online) (a) Hysteresis loops and (b) ΔM plots for samples with a 4 nm RL grown on $Mn_{67}Ru_{33}$ and Ru ILs. (c) TEM cross-sectional image of the sample with a 15 nm RL grown on $Mn_{67}Ru_{33}$ IL.

reveal well-isolated RL grains grown on the $Mn_{67}Ru_{33}$ IL [Fig. 4(b)] and poor RL grain separation on the Ru IL [Fig. 4(d)]. This shows that the MnRu IL can indeed promote SiO_2 segregation to the grain boundaries during the initial growth of the RL. This is also consistent with the reduced V_{act} of the 15-nm-thick RL on $Mn_{67}Ru_{33}$ IL.

Magnetic hysteresis loops and ΔM plots of samples with a 4 nm RL grown on $Mn_{67}Ru_{33}$ and Ru ILs are shown in Figs. 5(a) and 5(b), respectively. The samples grown on the Ru IL shows a square loop, typical of highly exchange-coupled grains.[8] A positive peak is found in the ΔM plot, also indicative of strong *exchange* coupling in the sample. In contrast, the sample deposited on the $Mn_{67}Ru_{33}$ IL exhibits decreased loop squareness and α; a negative peak is observed in the ΔM plot, indicating *dipolar* interactions between the grains of the RL. These results confirm that the MnRu IL can indeed enhance the RL grain isolation. Figure 5(c) shows the TEM cross-sectional image of a sample with 15 nm of RL grown on a $Mn_{67}Ru_{33}$ IL. Grain isolation is clearly observed through the $Mn_{67}Ru_{33}$ IL and into the RL.

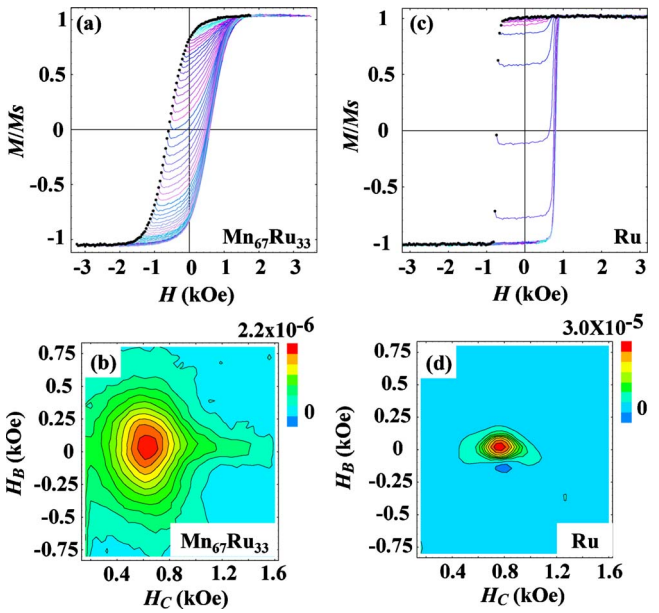

FIG. 6. (Color online) Families of FORCs, whose starting points are represented by black dots, are shown in (a) and (c) for samples with 4 nm of RL grown on $Mn_{67}Ru_{33}$ and Ru ILs, respectively. The corresponding FORC distributions are shown in (b) and (d).

Further evidence of the enhanced grain isolation is provided by the FORC analysis. Families of FORCs, along with the corresponding FORC distributions plotted in the (H_C, H_B) coordinate system are shown in Figs. 6(a)–6(d) for the samples with a 4 nm RL on $Mn_{67}Ru_{33}$ and Ru ILs, respectively. While both FORC distributions show a single peak, characteristic of a reversal via single-domain rotation,[24,25] the distribution is significantly broader in the sample with the $Mn_{67}Ru_{33}$ IL. The increased width along the H_C axis indicates a broad coercivity distribution while the enhanced width along the H_B axis indicates strong *dipolar-like* interactions between well-isolated grains, as confirmed by the TEM image shown in Fig. 4(b). Conversely, the TEM image of the sample with the Ru IL [Fig. 4(d)] shows poor grain separation, which results in strong *exchange* coupling between grains and a narrower FORC distribution along both H_C and H_B axes as shown in Fig. 6(d).

IV. CONCLUSIONS

In summary, microstructural, magnetometry, and FORC analyses demonstrate that a MnRu IL can both increase K_u and promote grain isolation in CoPtCr-SiO_2 perpendicular recording media. It is therefore an attractive replacement for the pure Ru IL. Although the effect of microstructure differences cannot be completely ruled out, the enhancement of the effective K_u of the RL is clearly attributable to the exchange bias provided by the adjacent AFM MnRu IL. The relatively separated grains in the MnRu IL, in turn, enhance grain isolation in the RL during the initial growth stage. While the enhanced grain isolation in the RL leads to a reduction in V_{act}, a potential loss in thermal stability is avoided due to the enhanced K_u.

ACKNOWLEDGMENTS

Work at NTHU has been supported by the National Science Council of Republic of China under Grant No. NSC 98-2622-E-007-003 and by the Ministry of Economic Affairs of Republic of China under Grant No. 97-EC-17-A-08-S1-006. Work at UCD has been supported in part by the National Science Foundation under Grant No. ECCS-0925626 and CITRIS.

*Corresponding author; chlai@mx.nthu.edu.tw

[1] R. Wood, J. Magn. Magn. Mater. **321**, 555 (2009).
[2] A. Moser, D. T. Margulies, and E. E. Fullerton, Phys. Rev. B **66**, 092410 (2002).
[3] F. C. S. da Silva and J. P. Nibarger, Phys. Rev. B **68**, 012414 (2003).
[4] D. Weller and A. Moser, IEEE Trans. Magn. **35**, 4423 (1999).
[5] Y. Liu, K. A. Dahmen, and A. Berger, Phys. Rev. B **77**, 054422 (2008).
[6] S. N. Piramanayagam, J. Appl. Phys. **102**, 011301 (2007).
[7] T. Hikosaka, U.S. Patent No. 006,670,056 B2 (2003).
[8] H. S. Jung, M. Kuo, S. S. Malhotra, and G. Bertero, Appl. Phys. Lett. **91**, 212502 (2007).
[9] U. Kwon, R. Sinclair, E. M. T. Velu, S. Malhotra, and G. Bertero, IEEE Trans. Magn. **41**, 3193 (2005).
[10] S. N. Piramanayagam, Appl. Phys. Lett. **89**, 162504 (2006).
[11] K. Srinivasan, S. N. Piramanayagam, and R. Sbiaa, Appl. Phys. Lett. **93**, 072503 (2008).
[12] J. E. Davies, O. Hellwig, E. E. Fullerton, G. Denbeaux, J. B. Kortright, and K. Liu, Phys. Rev. B **70**, 224434 (2004).
[13] M. T. Rahman, R. K. Dumas, N. Eibagi, N. N. Shams, Y. C. Wu, K. Liu, and C. H. Lai, Appl. Phys. Lett. **94**, 042507 (2009).
[14] P. J. Flanders and M. P. Sharrock, J. Appl. Phys. **62**, 2918 (1987).
[15] M. P. Sharrock, J. Appl. Phys. **76**, 6413 (1994).
[16] D. Suess, S. Eder, J. Lee, R. Dittrich, J. Fidler, J. W. Harrell, T. Schrefl, G. Hrkac, M. Schabes, N. Supper, and A. Berger, Phys. Rev. B **75**, 174430 (2007).
[17] M. Igarashi and Y. Sugita, IEEE Trans. Magn. **42**, 2399 (2006).
[18] P. E. Kelly, K. O'Grady, P. I. Mayo, and R. W. Chantrell, IEEE Trans. Magn. **25**, 3881 (1989).
[19] N. Honda, T. Kiya, and K. Ouchi, J. Magn. Soc. Jpn. **21**, 817 (1997).
[20] H. Yuan and D. E. Laughlin, J. Appl. Phys. **103**, 07F513 (2008).
[21] K. Liu, J. Nogues, C. Leighton, H. Masuda, K. Nishio, I. V. Roshchin, and I. K. Schuller, Appl. Phys. Lett. **81**, 4434 (2002).
[22] N. J. Gökemeijer, T. Ambrose, and C. L. Chien, Phys. Rev. Lett. **79**, 4270 (1997).
[23] P. H. Huang, C. H. Lai, C. A. Yang, H. H. Huang, T. S. Chin, C. H. Chen, M. D. Lan, H. E. Huang, and H. Y. Bor, IEEE Trans. Magn. **42**, 3014 (2006).
[24] R. K. Dumas, C. P. Li, I. V. Roshchin, I. K. Schuller, and K. Liu, Phys. Rev. B **75**, 134405 (2007).
[25] J. Wong, P. Greene, R. K. Dumas, and K. Liu, Appl. Phys. Lett. **94**, 032504 (2009).